Journal of Engineering Mathematics **38:** 141–154, 2000.

Nonlinear dynamic buckling of orthotropic cylindrical shells subjected to rapidly applied loads

DOO-SUNG LEE
Department of Mathematics (Education), Konkuk University, 93-1 Mojin-Dong, Kwangjin-Gu, Seoul, Korea
e-mail: dslee@kkucc.konkuk.ac.kr

Received 11 January 1999; accepted in revised form 28 July 1999.

Abstract. Dynamic buckling of an orthotropic cylindrical shell which is subjected to rapidly applied compression is considered. A nonlinear differential equation of Donnell–Karman type is derived with the initial imperfection taken into account. An energy method is used to obtain the equation of motion which is then solved numerically by means of a Runge-Kutta method. These numerical results show that the critical load is increased over the corresponding static case. An analytical solution is also obtained for the problem of hydrostatic pressure.

Key words: dynamic buckling, orthotropic cylindrical shell, energy method, buckling.

1. Introduction

Studies of structural dynamic instability began in the early 1950s. It is possible to classify the problems of dynamic instability according to the types of loading, and the features of the structural deformations during the instability process. Under such classification one group of problems is that where instability occurs under rapidly applied loads. A rapidly applied load differs from an impact load in that the time required to reach the critical load is greater than the time required for a pressure wave to travel from one end of the element to the other. Therefore, for a rapidly applied load, inertial effects in the middle plane of the element are negligible and only the motion normal to the middle surface needs to be considered.

The use of anistropic materials (both homogeneous and composite) has been increasing over the past years. Many applications involve shells and stiffened shells under loadings which cause failure by buckling. The dynamic stability of orthotropic cylindrical shells and stiffened shells which are treated as orthotropic ones if the stiffeners are densely placed has been analysed by numerous investigators and, recent and representative results are contained in [1–5]. In the present work, a circular orthotropic cylindrical shell, simply supported, subjected to a rapidly applied load is considered. Two cases are investigated in this analysis. One case is that the axial compressive loading is applied to the shell by a rigid testing machine, where the load is increased rapidly at a controlled rate. The other case is that the cylinder is subjected to a hydrostatic step pressure of infinite duration. Since the post-buckling behavior is to be considered, the large-deflection shell equations must be used. The effects of initial imperfections are also included. It has been known for many years that the presence of small physical or geometric imperfections in a given structure can lead to a decrease in its buckling strength. Such structures are called imperfection-sensitive. Hutchinson and Budiansky [6] formulated a general approximate theory of dynamic buckling of imperfection-sensitive structures by an extension of Koiter's static theory of post-buckling behaviour [7]. Lockhart [8, 9] and

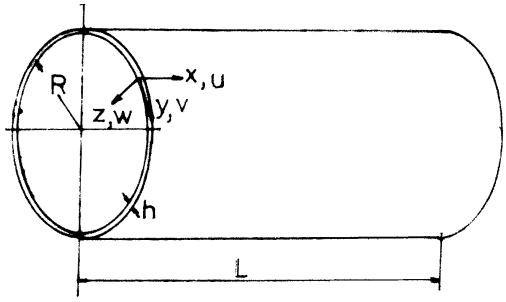

Figure 1. Shell geometry and coordinates.

Lockhart and Amazigo [10] studied the dynamic buckling of a finite cylinder subjected to a lateral or hydrostatic pressure in the form of a step-loading, a problem similar to the present one, by a perturbation technique.

Here we use an energy method. The Runge-Kutta method was used to obtain the numerical results. The analytical solution is derived for the problem of hydrostatic pressure and compared with the numerical solution.

2. Equations of motion

2.1. Axial compression

The nonlinear equations of motion are based on the assumptions commonly used in a Donnell-type formulation which is valid for a cylinder of moderate length. In the formulation of these equations the following assumptions are made:

(1) Donnell's nonlinear shell theory [11, pp. 200–201] is applicable;
(2) longitudinal and tangential inertia terms are of lower order of importance compared to normal inertia.

Figure 1 shows the cylindrical shell geometry and coordinate system. Let (u, v) represent the displacement components in the direction of the coordinate axes (x, y), respectively. The quantity w is the inward normal displacement. Also, the stress and strain components are denoted by $(\sigma_x, \sigma_y, \tau_{xy})$ and $(\varepsilon_x, \varepsilon_y, \gamma_{xy})$, respectively.

Assume that the natural axes of the material coincide with the coordinate axes, so that the middle-surface stress-strain relation may be written as

$$\begin{bmatrix} \sigma_x \\ \sigma_y \\ \tau_{xy} \end{bmatrix} = \frac{1}{1-\nu_{xy}\nu_{yx}} \begin{bmatrix} E_x & \nu_{xy}E_y & 0 \\ \nu_{yx}E_x & E_y & 0 \\ 0 & 0 & (1-\nu_{xy}\nu_{yx})G_{xy} \end{bmatrix} \begin{bmatrix} \varepsilon_x \\ \varepsilon_y \\ \gamma_{xy} \end{bmatrix}, \tag{1}$$

and

$$\begin{bmatrix} \varepsilon_x \\ \varepsilon_y \\ \gamma_{xy} \end{bmatrix} = \begin{bmatrix} 1/E_x & -\nu_{yx}/E_y & 0 \\ -\nu_{xy}/E_x & 1/E_y & 0 \\ 0 & 0 & 1/G_{xy} \end{bmatrix} \begin{bmatrix} \sigma_x \\ \sigma_y \\ \tau_{xy} \end{bmatrix}, \tag{2}$$

where E_x, E_y, and G_{xy} denote Young's moduli in the x- and y-directions and the shear modulus, respectively; ν_{xy} represents the relative contraction in the y-direction influenced by the tension in the x-direction. Apparently, the relation $E_x \nu_{yx} = E_y \nu_{xy}$ holds.

The critical load for a cylindrical shell under axial compression has been known to be sensitive to initial imperfections in the shell. In order to investigate the effect of the initial imperfections, one has to observe the post-buckling behavior and should include the second-order strain-displacement relations

$$\varepsilon_x = \frac{\partial u}{\partial x} + \frac{1}{2}\left(\frac{\partial w}{\partial x}\right)^2 - \frac{1}{2}\left(\frac{\partial w_0}{\partial x}\right)^2,$$

$$\varepsilon_y = \frac{\partial v}{\partial y} + \frac{1}{2}\left(\frac{\partial w}{\partial y}\right)^2 - \frac{1}{2}\left(\frac{\partial w_0}{\partial y}\right)^2 - \frac{w}{R} + \frac{w_0}{R}, \tag{3a, b, c}$$

$$\gamma_{xy} = \frac{\partial u}{\partial y} + \frac{\partial v}{\partial x} + \frac{\partial w}{\partial x}\frac{\partial w}{\partial y} - \frac{\partial w_0}{\partial x}\frac{\partial w_0}{\partial y}.$$

In (3) $w(x, y, t)$ is the total displacement normal to the middle surface and $w_0(x, y)$ is the initial displacement normal to the middle surface.

Now, one may represent the stress components in terms of a stress function $F(x, y, t)$ in the form as

$$\sigma_x = \frac{\partial^2 F}{\partial y^2}, \qquad \sigma_y = \frac{\partial^2 F}{\partial x^2}, \qquad \tau_{xy} = -\frac{\partial^2 F}{\partial x\, \partial y}. \tag{4a, b, c}$$

These automatically satisfy the equations of equilibrium in the plane tangent to the middle surface of the shell when the body force is not included. Then, the compatibility equation yields

$$\frac{\partial^4 F}{\partial x^4} + \left(\frac{E_y}{G_{xy}} - 2\nu_{xy}\frac{E_y}{E_x}\right)\frac{\partial^4 F}{\partial x^2 \partial y^2} + \frac{E_y}{E_x}\frac{\partial^4 F}{\partial y^4}$$

$$= E_y\left[\left(\frac{\partial^2 w}{\partial x\, \partial y}\right)^2 - \frac{\partial^2 w}{\partial x^2}\frac{\partial^2 w}{\partial y^2} - \frac{1}{R}\frac{\partial^2 w}{\partial x^2} - \left(\frac{\partial^2 w_0}{\partial x\, \partial y}\right)^2\right.$$

$$\left. + \frac{\partial^2 w_0}{\partial x^2}\frac{\partial^2 w_0}{\partial y^2} + \frac{1}{R}\frac{\partial^2 w_0}{\partial x^2}\right]. \tag{5}$$

The deflection function $w(x, y, t)$ is chosen in the separable form

$$w(x, y, t) = f(t) \sin\left(\frac{m\pi x}{L}\right) \sin\left(\frac{ny}{R}\right), \tag{6}$$

where $f(t)$ is the time-varying amplitude of w, and m and n represent the number of longitudinal half-wave and circumferential waves, respectively.

In analyzing the effects of initial imperfections, one usually assumes the initial and final shapes to be of the same basic form. Thus, the initial shape of the cylindrical shell will be taken as

$$w_0(x, y) = f_0 \sin\left(\frac{m\pi x}{L}\right) \sin\left(\frac{ny}{R}\right), \tag{7}$$

where f_0 is the amplitude. This also satisfies the boundary conditions.

Substitution of (6) and (7) in the compatibility equation (5) yields a particular solution for a cylinder under the compressive pressure σ_0 only

$$F(x, y, t) = E_y \left[\frac{\beta^2}{32m^2}(f^2 - f_0^2) \cos\left(\frac{2m\pi x}{L}\right) + \frac{m^2}{32k^2\beta^2}(f^2 - f_0^2) \cos\left(\frac{2ny}{R}\right) + \frac{m^2 L^2 (f - f_0)}{R\pi^2(m^4 + b^2m^2\beta^2 + k^2\beta^4)} \sin\left(\frac{m\pi x}{L}\right) \sin\left(\frac{ny}{R}\right) \right] - \sigma_0 \frac{y^2}{2}, \tag{8}$$

where σ_0 is defined as the average value of the compressive stress in the x-direction, and

$$b^2 = \frac{E_y}{G_{xy}} - 2\nu_{xy}\frac{E_y}{E_x}, \qquad k^2 = \frac{E_y}{E_x} = \frac{D_y}{D_x}, \qquad \beta = \frac{nL}{\pi R}. \tag{9}$$

In Donnell's theory the 'stretching' displacement v resulting from the changes of curvature and twist is neglected. Thus, the moment can be expressed as

$$\begin{aligned} M_x &= -\left[D_x \frac{\partial^2 \bar{w}}{\partial x^2} + D_y \nu_{yx} \frac{\partial^2 \bar{w}}{\partial y^2} \right], \qquad M_y = -\left[D_y \frac{\partial^2 \bar{w}}{\partial y^2} + D_x \nu_{xy} \frac{\partial^2 \bar{w}}{\partial x^2} \right], \\ M_{xy} &= M_{yx} = -G_{xy} \frac{h^3}{6} \frac{\partial^2 \bar{w}}{\partial x\, \partial y}, \end{aligned} \tag{10}$$

where

$$\bar{w} = w - w_0, \qquad D_x = E_x \frac{h^3}{12(1 - \nu_{xy}\nu_{yx})}, \qquad D_y = E_y \frac{h^3}{12(1 - \nu_{xy}\nu_{yx})}. \tag{11}$$

Equations (10) are identical to the corresponding equations which appear in the theory of plates [12]. From (10) the strain energy due to the bending can be written as

$$U_1 = \frac{1}{2} \int\int_S \left[D_x \left(\frac{\partial^2 \bar{w}}{\partial x^2}\right)^2 + D_y \left(\frac{\partial^2 \bar{w}}{\partial y^2}\right)^2 + (D_x \nu_{xy} + D_y \nu_{yx}) \frac{\partial^2 \bar{w}}{\partial x^2} \frac{\partial^2 \bar{w}}{\partial y^2} + 2G_{xy} \frac{h^3}{6} \left(\frac{\partial^2 \bar{w}}{\partial x\, \partial y}\right)^2 \right] \mathrm{d}x\, \mathrm{d}y. \tag{12}$$

where S denotes the surface of the cylindrical shell. Putting (6) and (7) into (12) and performing integration, we obtain

$$U_1 = P A_1 (f - f_0)^2, \tag{13}$$

where

$$P = \pi\rho h R L/4, \qquad A_1 = \frac{D_x}{\rho h} \left(\frac{\pi}{L}\right)^4 (m^4 + k^2\beta^4 + 2\beta^2 m^2 c^2), \tag{14}$$

with

$$c^2 = \frac{1}{D_x} \left[\tfrac{1}{2}(D_x \nu_{xy} + D_y \nu_{yx}) + \frac{h^3}{6} G_{xy} \right]. \tag{15}$$

In (14) ρ is the mass density of the shell material. Using (2) and (4) we can write the strain energy due to the stretching of the middle plane as

$$U_2 = \frac{h}{2}\int\int_S (\sigma_x\varepsilon_x + \sigma_y\varepsilon_y + \tau_{xy}\gamma_{xy})\,\mathrm{d}x\,\mathrm{d}y = \frac{h}{2}\int\int_S \left[\frac{1}{E_x}\left(\frac{\partial^2 F}{\partial y^2}\right)^2 + \frac{1}{E_y}\left(\frac{\partial^2 F}{\partial x^2}\right)^2 - \left(\frac{\nu_{xy}}{E_x} + \frac{\nu_{yx}}{E_y}\right)\frac{\partial^2 F}{\partial x^2}\frac{\partial^2 F}{\partial y^2} + \frac{1}{G_{xy}}\left(\frac{\partial^2 F}{\partial x\,\partial y}\right)^2\right]\mathrm{d}x\,\mathrm{d}y. \tag{16}$$

Substituting from (8) in (16), we find

$$U_2 = P\left[\frac{H}{2}(f^2 - f_0^2)^2 + A_2(f - f_0)^2 + \frac{4\sigma_0^2}{\rho E_x}\right], \tag{17}$$

where

$$H = \frac{E_y}{16\rho}\left(\frac{\pi}{L}\right)^4 \frac{m^4 + k^2\beta^4}{k^2}, \qquad A_2 = \frac{E_y}{\rho R^2}\frac{m^4}{(m^4 + b^2m^2\beta^2 + k^2\beta^4)}. \tag{18a, b}$$

Next we consider the work done by the compressive force. Using for the axial strain before buckling the notation

$$\varepsilon_0 = -\frac{\sigma_0}{E_x}, \tag{19}$$

we obtain

$$\varepsilon_x + \nu_{yx}\varepsilon_y = \varepsilon_0(1 - \nu_{xy}\nu_{yx}). \tag{20}$$

Observing that

$$\varepsilon_y = -\nu_{xy}\varepsilon_0 - \frac{w}{R} + \frac{w_0}{R} = -\nu_{xy}\varepsilon_0 - \frac{1}{R}(f - f_0)\,\sin\left(\frac{m\pi x}{L}\right)\sin\left(\frac{ny}{R}\right), \tag{21}$$

we find

$$\varepsilon_x - \varepsilon_0 = \nu_{yx}\left(\frac{w}{R} - \frac{w_0}{R}\right) = \nu_{yx}\frac{1}{R}(f - f_0)\,\sin\left(\frac{m\pi x}{L}\right)\sin\left(\frac{ny}{R}\right).$$

The work done by the compressive forces during buckling is

$$U_3 = -\sigma_0 h\int_0^{2\pi R}\int_0^L \left[\varepsilon_x - \varepsilon_0 + \frac{1}{2}\left\{\left(\frac{\partial w}{\partial x}\right)^2 - \left(\frac{\partial w_0}{\partial x}\right)^2\right\}\right]\mathrm{d}x\,\mathrm{d}y$$

$$= -(f^2 - f_0^2)\frac{\sigma_0}{\rho}\frac{m^2\pi^2}{L^2}P. \tag{22}$$

The kinetic energy is

$$K = \tfrac{1}{2}h\rho\int\int_S (\dot{w})^2\,\mathrm{d}x\,\mathrm{d}y = P\{\dot{f}(t)\}^2, \tag{23}$$

where the dot denotes differentiation with respect to time t. We define now the Lagrangian function

$$\begin{aligned} L &= K - U_1 - U_2 - U_3 \\ &= P\left[\{\dot{f}(t)\}^2 - A(f-f_0)^2 - B(f^2-f_0^2) - \frac{H}{2}(f^2-f_0^2)^2 - \frac{4\sigma_0^2}{E_x\rho}\right], \end{aligned} \tag{24}$$

where

$$A = A_1 + A_2, \qquad B = -\frac{\sigma_0}{\rho}\frac{m^2\pi^2}{L^2}. \tag{25}$$

The Euler–Lagrange equation for $f(t)$ associated with the above Lagrangian (24) is obtained from

$$\frac{\mathrm{d}}{\mathrm{d}t}\left(\frac{\partial L}{\partial \dot{f}}\right) - \frac{\partial L}{\partial f} = 0. \tag{26}$$

Substituting from (24) in (26), we obtain the Euler–Lagrange equation for f

$$\frac{\mathrm{d}^2 f}{\mathrm{d}t^2} + A(f-f_0) + Bf + H(f^2-f_0^2)f = 0. \tag{27}$$

Omitting the inertia and nonlinear terms and setting $f_0 = 0$, then we have that the resulting equation is the corresponding static buckling equation using the linear theory which yields the critical compressive stress

$$\begin{aligned} \sigma_{\mathrm{cr}} &= \frac{\pi^2 E_x}{12(1-\nu_{xy}\nu_{yx})}\left(\frac{h}{L}\right)^2\left[\frac{(m^4+k^2\beta^4+2\beta^2m^2c^2)}{m^2} + \frac{12(1-\nu_{xy}\nu_{yx})k^2L^4}{\pi^4R^2h^2}\right. \\ &\qquad \left.\times\frac{m^2}{(m^4+b^2m^2\beta^2+k^2\beta^4)}\right]. \end{aligned} \tag{28}$$

If the shell is isotropic, then $\nu_{xy} = \nu_{yx} = \nu$, $E_x = E_y = E$, $c^2 = 1$, $k^2 = 1$, $b^2 = 2$, and (28) becomes

$$\frac{\sigma_{\mathrm{cr}}(1-\nu^2)}{E} = \frac{h^2}{12R^2}\frac{(\lambda^2+n^2)^2}{\lambda^2} + \frac{(1-\nu^2)\lambda^2}{(\lambda^2+n^2)^2}, \tag{29}$$

where

$$\lambda = \frac{m\pi R}{L}. \tag{30}$$

Equation (29) is exactly the same as the one from the classical linear theory [12, pp. 464–465].

The large-deflection equation describing the static post-buckling behavior is obtained by omitting $\mathrm{d}^2 f/\mathrm{d}t^2$ term from (27) with $f_0 = 0$

$$\begin{aligned} &\left[\frac{D_x}{h}\left(\frac{\pi}{L}\right)^4(m^4+k^2\beta^4+2\beta^2m^2c^2) + \frac{E_y}{R^2}\frac{m^4}{(m^4+b^2m^2\beta^2+k^2\beta^4)} - \sigma_0\frac{m^2\pi^2}{L^2}\right] \\ &\quad + \frac{\pi^4E_y}{16L^4}\frac{(m^4+k^2\beta^4)}{k^2}f^2 = 0. \end{aligned} \tag{31}$$

For real values of f, the quantity in the bracket should be negative.

As an example of the solution of (27), consider the case where the average compressive stress increases linearly with time; $\sigma_0 = c_0 t$. The equation of motion, (27), will have a more convenient form if the following nondimensional parameters are introduced.

$$\zeta = \frac{f}{h}, \qquad \zeta_0 = \frac{f_0}{h}, \qquad \tau = \frac{\sigma_0}{\sigma_{cr}} = \frac{c_0 t}{\sigma_{cr}}, \qquad S = \frac{\sigma_{cr}^3 \pi^2}{\rho L^2 c_0^2} m^2. \tag{32}$$

With these substitutions, (27) becomes

$$\frac{d^2\zeta}{d\tau^2} + S\left[\zeta - \zeta_0 + \frac{\pi^2 h^2}{16L^2}\frac{E_x}{\sigma_{cr}}\frac{(m^4 + k^2\beta^4)}{m^2}(\zeta^2 - \zeta_0^2)\zeta - \tau\zeta\right] = 0. \tag{33}$$

2.2. Hydrostatic pressure

In this section, we consider the case when the cylinder is subject to a hydrostatic pressure. This analysis is particularly applicable in constructing submarine vessels of anisotropic materials, the prospect of which led to the recent surge in interest in the compressive failure of anisotropic cylinders. For the present case, a little modification is necessary in (8). The last term $-\sigma_0 y^2/2$ is to be replaced by $-\sigma_0 x^2/2$ with σ_0 being the circumferential compressive stress, $\sigma_0 = qR/h$, where q is the external hydrostatic pressure. This leads us to replace $4\sigma_0^2/\rho E_x$, the last term of (17), by $4\sigma_0^2/\rho E_y$. The work done by the circumferential compressive force is now

$$\begin{aligned} U_3 &= -\sigma_0 h \int_0^{2\pi R}\int_0^L \left[-\frac{w}{R} + \frac{w_0}{R} + \frac{1}{2}\left\{\left(\frac{\partial w}{\partial y}\right)^2 - \left(\frac{\partial w_0}{\partial y}\right)^2\right\}\right] dx\, dy \\ &= -\frac{\sigma_0}{\rho}\left(\frac{n}{R}\right)^2 P(f^2 - f_0^2). \end{aligned} \tag{34}$$

Equation (27) remains unchanged, except that B is now replaced by

$$B = -\frac{\sigma_0}{\rho}\left(\frac{n}{R}\right)^2. \tag{35}$$

The critical stress obtained from the static buckling equation of linear theory when $f_0 = 0$, is then

$$\sigma_{ycr} = \frac{m^2}{\beta^2}\sigma_{cr}, \tag{36}$$

where σ_{cr} is given by (28). If the shell is isotropic, Equation (36) becomes

$$\sigma_{ycr} = \frac{\pi^2 E}{12(1-\nu^2)}\left(\frac{h}{L}\right)^2\left[\frac{(m^2+\beta^2)^2}{\beta^2} + \frac{12Z^2}{\pi^4}\frac{m^4}{\beta^2(m^2+\beta^2)^2}\right], \tag{37}$$

where $Z = L^2\sqrt{1-\nu^2}/Rh$. Equation (37) is exactly the same that obtained from the classical linear theory [13]. As an example of (27), we consider the case when the cylinder is subjected to a step pressure of infinite duration. Its time variation is considered as

$$q = 0 \quad \text{when} \quad t < 0, \qquad q = q_0 \quad \text{when} \quad t \geqslant 0.$$

Unlike the example considered in the previous section, we can solve this problem analytically in terms of elliptic integrals. The nondimensional parameter for t in (32) is not suitable for the present case, and we set

$$\tau = \frac{1}{R}\sqrt{\frac{E_x}{\rho}}t, \qquad p = \frac{q_0}{p_{\rm cr}}, \tag{38}$$

where $p_{\rm cr} = \sigma_{y{\rm cr}}h/R$. With these substitutions, Equations (27) becomes

$$\dot{\zeta} + \mathcal{A}(\zeta - \zeta_0 - p\zeta) + \mathcal{B}(\zeta^2 - \zeta_0^2)\zeta = 0, \tag{39}$$

where

$$\mathcal{A} = n^2\frac{p_{\rm cr}}{E_x}\frac{R}{h}, \qquad \mathcal{B} = \frac{\pi^4 R^2 h^2}{16L^4}(m^4 + k^2\beta^4). \tag{40}$$

After multiplying (39) with $\dot{\zeta}$ and integrating the resulting equation and using the initial condition

$$\ddot{\zeta} = 0, \qquad \zeta = \zeta_0, \quad \text{when} \quad \tau = 0,$$

we obtain

$$\dot{\zeta}^2 = -\mathcal{A}(\zeta - \zeta_0)^2 + \mathcal{A}p(\zeta^2 - \zeta_0^2) - \frac{\mathcal{B}}{2}(\zeta^2 - \zeta_0^2)^2. \tag{41}$$

Let us write (41) as

$$\dot{\zeta}^2 = \frac{\mathcal{B}}{2}(-\zeta^4 + a_1\zeta^2 + a_2\zeta - a_3) = \frac{\mathcal{B}}{2}(-\zeta^2 + 2d\zeta + c_1)(\zeta^2 + 2d\zeta + c_2), \tag{42}$$

where

$$\begin{aligned} &a_1 = 2\{\zeta_0^2 + \mathcal{C}(p-1)\}, \qquad a_2 = 4\zeta_0\mathcal{C}, \\ &a_3 = \{\zeta_0^2 + 2\mathcal{C}(p+1)\}\zeta_0^2, \qquad \mathcal{C} = \mathcal{A}/\mathcal{B}. \end{aligned} \tag{43}$$

Then $b_1\ (= d^2)$ satisfies following cubic equation

$$b_1^3 - \frac{a_1}{2}b_1^2 + \left\{\left(\frac{a_1}{4}\right)^2 - \frac{a_3}{4}\right\}b_1 - \frac{a_2^2}{64} = 0. \tag{44}$$

After solving (44), using the Cardano equation for correct solution, we find that it is appropriate to choose $d = -\sqrt{b_1}$. Having obtained d, we get the following results for c_1 and c_2

$$c_1 = \frac{1}{2}\left(\frac{a_2}{2d} + a_1 - 4d^2\right), \qquad c_2 = \frac{1}{2}\left(\frac{a_2}{2d} - a_1 + 4d^2\right). \tag{45}$$

Let

$$S_1 = -\zeta^2 + 2d\zeta + c_1, \qquad S_2 = \zeta^2 + 2d\zeta + c_2, \tag{46}$$

then

$$S_1 - \xi S_2 = -(1+\xi)\zeta^2 + 2d(1-\xi)\zeta + (c_1 - \xi c_2). \tag{47}$$

Equation (47) will become a perfect square in ζ if the following equation is satisfied

$$(1+\xi)(c_1 - \xi c_2) + (1-\xi)^2 d^2 = 0. \tag{48}$$

Let the two roots of the quadratic equation (48) be ξ_1 and ξ_2; then

$$S_1 - \xi_1 S_2 = -(1+\xi_1)(\zeta - \alpha)^2, \qquad S_1 - \xi_2 S_2 = -(1+\xi_2)(\zeta - \gamma)^2, \tag{49}$$

where

$$\alpha = \frac{1-\xi_1}{1+\xi_1} d, \qquad \gamma = \frac{1-\xi_2}{1+\xi_2} d.$$

On solving (49) as equation in S_1, S_2, we obviously get the results

$$S_1 = \frac{1}{\xi_1 - \xi_2}[C_1(\zeta - \alpha)^2 - D_1(\zeta - \gamma)^2], \quad S_2 = \frac{1}{\xi_1 - \xi_2}[C_2(\zeta - \alpha)^2 - D_2(\zeta - \gamma)^2], \tag{50}$$

where

$$C_1 = \xi_2(1+\xi_1), \qquad D_1 = \xi_1(1+\xi_2), \qquad C_2 = 1+\xi_1, \qquad D_2 = 1+\xi_2. \tag{51}$$

In (41), let us take a new variable T defined by the equation,

$$T = -\frac{\zeta - \alpha}{\zeta - \gamma}. \tag{52}$$

We then have

$$\mathrm{d}\tau = \pm \frac{(\xi_1 - \xi_2)\sqrt{2}}{(\alpha - \gamma)\sqrt{\mathcal{B}}} \frac{\mathrm{d}T}{\sqrt{D_1 - C_1 T^2}\sqrt{D_2 - C_2 T^2}}. \tag{53}$$

Again, by physical reasoning, the negative sign is chosen in (53). In (53) we put $T = \sqrt{D_2/C_2}\cos\varphi$, and then integrate it. There are two cases:

(1) if $p > p_0$ (say), then $C_1 > 0$,
(2) if $p < p_0$, then $C_1 < 0$.

In case (1), we have

$$\tau = F_1 \int_0^{\phi} \frac{\mathrm{d}\varphi}{\sqrt{1 - k^2 \cos^2 \varphi}}, \tag{54}$$

where

$$F_1 = \frac{(\xi_1 - \xi_2)\sqrt{2}}{(\alpha - \gamma)\sqrt{\mathcal{B} C_2 D_1}}, \qquad k = \left(\frac{C_1 D_2}{C_2 D_1}\right)^{1/2}.$$

In case (2), we have

$$\tau = F_2 \int_0^{\phi} \frac{\mathrm{d}\varphi}{\sqrt{1 - k^2 \sin^2 \varphi}}, \tag{55}$$

where

$$F_2 = \frac{(\xi_1 - \xi_2)\sqrt{2}}{(\alpha - \gamma)\sqrt{\mathcal{B}(C_2 D_1 - C_1 D_2)}}, \qquad k = \left(\frac{C_1 D_2}{C_1 D_2 - C_2 D_1}\right)^{1/2}.$$

In (54) and (55), if we put $\phi = \pi/2$, we obtain

$$\mathcal{T} = 4F_i K(k) \quad (i = 1, 2). \tag{56}$$

In (56) $\mathcal{T}$ is the period of one cycle and $K(k)$ is the complete elliptic integral of the first kind. The nondimensional deflection ζ can be obtained from (52) as

$$\zeta = \frac{\alpha + \gamma e \cos\varphi}{1 + e \cos\varphi}, \tag{57}$$

where $e = \sqrt{D_2/C_2}$. If p is less than some value which is smaller than p_0, we have the solution of imaginary ζ.

If U_T denotes the total potential energy, the dynamic buckling can be obtained from the condition [14, 15, 16]

$$U_T = 0, \qquad \frac{\mathrm{d}U_T}{\mathrm{d}\zeta} = 0. \tag{58a, b}$$

The dynamic instability occurs [14] when

$$\frac{\mathrm{d}\zeta}{\mathrm{d}p} = \infty. \tag{59}$$

Condition (58b) is obtained from (59). We do not find such point where (59) holds. The reason is as follows. First, note that the right-hand side of (41) is proportional to U_T. Thus, if we solve (58a) and (58b) simultaneously, we obtain the following equation.

$$\mathcal{B}(\zeta - \zeta_0)^2(\zeta + \zeta_0) = -2\mathcal{A}p\zeta_0.$$

We can immediately see that there are no positive values of ζ which satisfy the above equation. A relaxed condition for the present problem will be

$$\frac{\mathrm{d}\zeta}{\mathrm{d}p} = \max. \tag{60}$$

Solving (58a) and (60), we obtain as the maximum deflection $\bar{\zeta}$ at the point where the rate of increment is at a maximum

$$\bar{\zeta} = \sqrt[3]{4\zeta_0 \mathcal{C}} - \zeta_0. \tag{61}$$

Table 1. Material properties.

$E_x = 40 \times 10^6$psi,	$\nu_{yx} = 0{\cdot}025$,
$E_y = 4 \times 10^6$psi,	$k^2 = 0{\cdot}1$,
$G_{xy} = 1{\cdot}5 \times 10^6$psi,	$c^2 = 0{\cdot}0995$,
$\nu_{xy} = 0{\cdot}25$,	$b^2 = 2{\cdot}66167$.

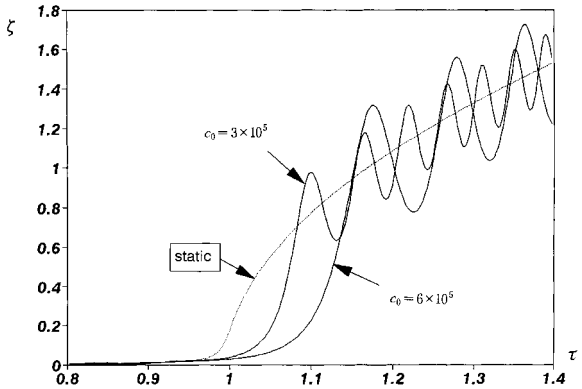

Figure 2. Response curves for $\zeta_0 = 0{\cdot}001$.

Then we have for p

$$p = 1 - (2\zeta_0^2 \mathcal{C})^{2/3}. \tag{62}$$

3. Numerical examples

To illustrate the application of (33), numerical solutions are made for boron/epoxy cylindrical shells of various geometries and at several loading rates. The material properties used are shown in Table 1. The specific weight of the shell is $0{\cdot}0585\,\mathrm{lb/in^3}$.

3.1. Axial compression

Numerical results are presented for the cylindrical shell $R/h = 100$, $l/R = 2$, and $h = 0{\cdot}1$ in. Equation (33) was solved numerically by means of a variable-step fourth-order Runge-Kutta method. The critical load is at a maximum when $m = 1$. Assuming that the mode shapes of the linear problem are also relevant in the nonlinear problem of imperfect cylinders, we choose the critical number of circumferential waves as 6[12, pp. 474–82] and an asymmetric mode with $m = 1$ is selected in the numerical calculation. Three values of $\zeta_0 - 0{\cdot}001, 0{\cdot}005$, and $0{\cdot}01$ and two values of $c_0 - 300{,}000$ psi/sec and 600,000 psi/sec were used. The initial conditions for the problem are $\zeta = \zeta_0$ and $\mathrm{d}\zeta/\mathrm{d}\tau = 0$ at $\tau = 0$. The numerical solution of (33) are plotted in Figures 2–6 with the static solution included for comparison. Each shows that there is initially a relatively slow increase of deflection, then a rapid increase, and finally a series of nonlinear oscillations.

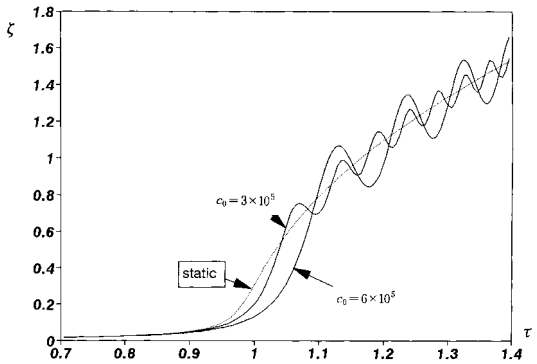

Figure 3. Response curve for $\zeta_0 = 0{\cdot}005$.

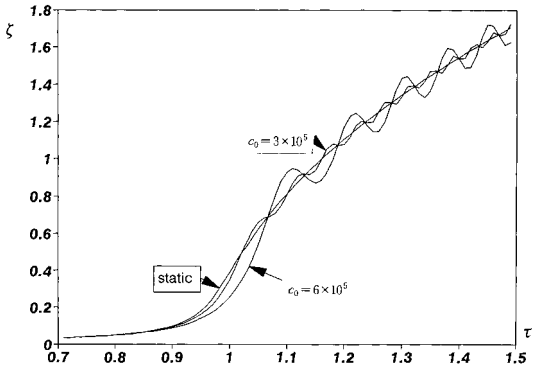

Figure 4. Response curves for $\zeta_0 = 0{\cdot}01$.

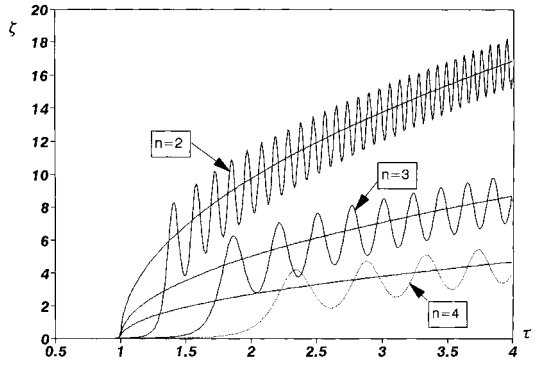

Figure 5. Response curves for various values of n, $\zeta_0 = 0{\cdot}001$, $m = 1$.

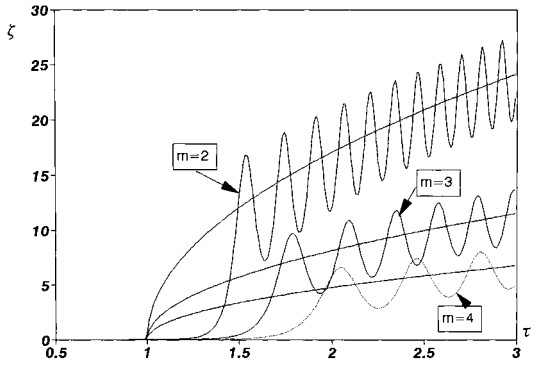

Figure 6. Response curves for various values of m, $\zeta_0 = 0{\cdot}001$, $n = 1$.

These figures show the effect of the two loading rates on the response of shells having the same initial imperfections. In each case the response curve for the faster loading rate ($c_0 = 6 \times 10^5$) is to the right of that for the slower ($c_0 = 3 \times 10^5$). An examination of Figure 2 shows that there is no definite point of instability as in static analyses. Rather, there is a region of instability where the slope of the ζ *vs.* τ curve increases rapidly. For $c_0 = 3 \times 10^5$ this region is between $\tau = 1{\cdot}03$ and $\tau = 1{\cdot}05$, while for $c_0 = 6 \times 10^5$ it is between $\tau = 1{\cdot}06$ and $\tau = 1{\cdot}1$. Both response curves oscillate about the static response curve with increasing frequency. At any value of τ, the frequency for $c_0 = 6 \times 10^5$ is less than that for $c_0 = 3 \times 10^5$. The amplitude of the oscillations, relative to the static curve, is greater for the faster loading rate than for the slower. These oscillations result from the release of part of the strain energy stored in the cylinder before buckling when the deflection is zero or very small. The time to reach the region of instability is less for the slower rate and hence less strain energy is stored before buckling. In Figure 3, the situation is very similar to that shown in Figure 2. In Figure 4 we notice that the curve for the slower loading rate is very similar to the static curve.

In Figure 5 we have plotted response curves for different values of n, while m is fixed to 1. When $n = 2$, the oscillation is most frequent, and we can notice from this figure that, as n increases, the frequency as well as the deflection decrease and the region of instability appears later, while the static instability occurs around $\tau = 1$ for all values of n. In Figure 5, values are chosen as $R/h = 50$, $L/R = 2$, and $c_0 = 10^8$ psi/sec. In Figure 6, we show response

Table 2. Critical values of pressure ratio.

Initial imperfection	p_{cr}
0·0005	0·99999
0·001	0·99998
0·005	0·99986
0·01	0·99965

curves when $R/h = 150$. Other values are same as in Figure 5. We can see that the situation is similar to that of Figure 5 with the roles of m and n being reversed.

3.2. HYDROSTATIC STEP LOAD

In the numerical example, the number of circumferential waves n and longitudinal half-waves m are chosen to be 6 and 1, respectively. The deflection response curves are plotted from the analytical solution given by (57). In Figure 7 the typical response curves of the orthotropic cylindrical shell under step pressure are shown.

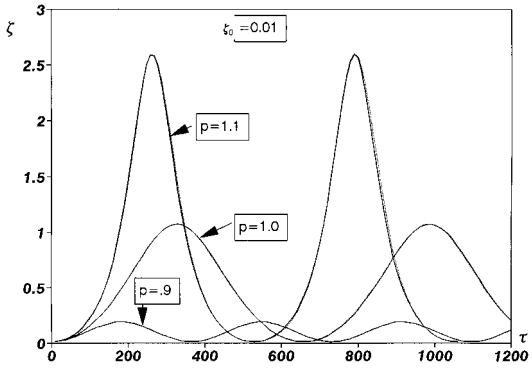

Figure 7. Nonlinear response curves of the cylindrical shell under step pressure.

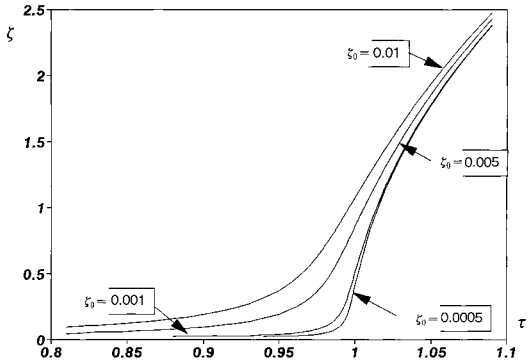

Figure 8. Amplitude load curves for a cylindrical shell under step pressure.

The numerical solution of (39) is also obtained by means of the fourth-order Runge-Kutta method and compared with the analytical solution shown in Figure 7. The solid line is obtained from the analytical solution and the dotted line from the numerical solution. The agreement between two solutions is so excellent that the two curves are almost indistinguishable. An examination of Figure 7 shows that there is no definite change of stability. Since $\mathcal{B}$ in (39) is positive, all solutions are bounded and periodic [9]. It is worth observing that the system becomes dynamically stable for loads much higher than the dynamic buckling load, above a certain level. This is called the metastability phenomenon [17]. In Figure 8 amplitude load curves are shown.

Table 2 shows the critical values of the ratios between the dynamic pressure and the static pressure on orthotropic cylindrical shells as calculated from (62).

4. Conclusions

In the present work two types of loading are considered and the results of the investigation may be summarized as follows:

When the shell is subjected to axial compression at a controlled rate

(1) A cylindrical shell compressed rapidly will buckle at a higher critical stress than a cylindrical shell compressed very slowly.
(2) The amplitude of oscillations increases as the loading rate is increased.
(3) Initial imperfections decrease the critical stress and the amplitude of postbuckling oscillations.
(4) For a fixed $m(n)$, as $n(m)$ increases, the critical stress increases, while the amplitude of postbuckling oscillations decreases.

When the shell is subjected to the hydrostatic step loading of infinite duration

(1) All solutions are bounded and periodic.
(2) When the critical loads are obtained from the condition (60), we notice that the effect of initial imperfection on the cylindrical shell is not very significant.
(3) The dynamic buckling load can be approximated by the static buckling load, if the condition (60) is applied.

References

1. A. Schokker, A. Kasagi and S. Sridharan, Dynamic interactive buckling of ring stiffened composite shells. *AIAA J.* 33 (1995) 1954–1962.
2. T. C. K. Molyneaux and L.-Y. Li, Dynamic elastic instability of long circular cylindrical shells under pure bending. *Thin-Walled Structures* 24 (1996) 123–133.
3. B. Yang and J. Zhou, Analysis of ring-stiffened cylindrical shells. *J. Appl. Mech.* 62 (1995) 1005–1014.
4. B. Budiansky and C. Amazigo, Initial post buckling behavior of cylindrical shells under external pressure. *J. Math. Phys.* 47 (1968) 223–235.
5. D. I. Anderson and H. E. Lindberg, Dynamic pulse buckling of cylindrical shells under lateral pressure. *AIAA J.* 6 (1968) 589–598.
6. J. W. Hutchinson and B. Budiansky, Dynamic buckling estimates. *AIAA J.* 4 (1966) 525–530.
7. W. T. Koiter, Elastic stability and postbuckling behavior. In: R. E. Langer (ed.), *Nonlinear Problems.* Madison (Wisc.): U. Wisconsin Press (1963) pp. 257–275.
8. D. F. Lockhart, Dynamic buckling of a damped externally pressurized imperfect cylindrical shell. *J. Appl. Mech.* 46 (1979) 372–376.
9. D. F. Lockhart, Postbuckling dynamic behavior of periodically supported imperfect shells. *Int. J. Non- Linear Mech.* 17 (1982) 165–174.
10. D. F. Lockhart and J. C. Amazigo, Dynamic buckling of externally pressurized imperfect cylindrical shells. *J. Appl. Mech.* 42 (1975) 316–320.
11. H. Kraus, *Thin Elastic Shells.* New York: John Wiley (1967) 476pp.
12. S. Timoshenko and J. M. Gere, *Elastic Stability*. New York: McGraw-Hill (1961) 541pp.
13. G. Gerard, *Introduction to Structural Stability Theory*. New York: McGraw-Hill (1962) 170pp.
14. A. N. Kounadis, J. Mallis and J. Raftoyiannis, Dynamic buckling estimates for discrete systems under step loading. *Z. angew. Math. Mech.* 17 (1991) 391–402.
15. A. N. Kounadis, Nonlinear dynamic buckling of discrete dissipative or nondissipative systems under step loading. *AIAA J.* 29 (1991) 280–289.
16. B. Wu, A method for determining the lower bound dynamic buckling loads of imperfection-sensitive structures. *Z. angew. Math. Mech.* 77 (1997) 447–456.
17. A. N. Kounadis, Nonlinear dynamic buckling and stability of autonomous structural systems. *Int. J. Mech. Sci.* 35 (1993) 643–656.